The Abdus Salam
International Centre for Theoretical Physics

United Nations
Educational, Scientific
and Cultural Organization

International Atomic
Energy Agency

SMR 1666 - 4

SCHOOL ON QUANTUM PHASE TRANSITIONS AND NON-EQUILIBRIUM PHENOMENA IN COLD ATOMIC GASES

11 - 22 July 2005

Experiments with Fermions in Optical Lattices

Presented by:

Michael Köhl

Institute of Quantum Electronics, Zurich

Experiments with Fermions in Optical Lattices

Michael Köhl, Thilo Stöferle, Henning Moritz, Kenneth Günter, Tilman Esslinger

Institute of Quantum Electronics, ETH Zürich Hönggerberg, CH–8093 Zürich, Switzerland
Email: koehl@phys.ethz.ch, Web: www.quantumoptics.ethz.ch

(Dated: 19.7.2005)

In this lecture I will discuss experiments with interacting and non-interacting fermions in 3D optical lattices.

I. INTRODUCTION

Fermions in optical lattices give access to few-body and many-body quantum physics.

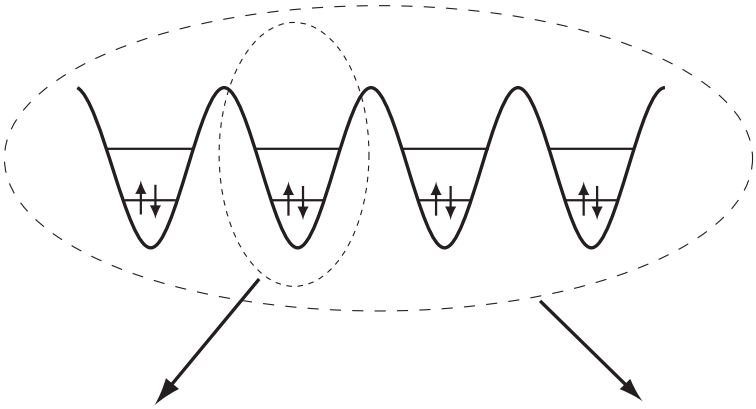

FIG. 1 Principal physics in an optical lattice.

In a **single lattice well** the atoms constitute a few body system which can be described by the Hamiltonian (1)

$$H = \sum_i \left(-\frac{\hbar^2}{2m}\nabla_i^2 + \frac{m\omega^2}{2}\mathbf{r}_i^2 \right) + \frac{4\pi\hbar^2 a}{m}\delta(\mathbf{r}_1 - \mathbf{r}_2)\frac{\partial}{\partial r} r.$$

ω quantifies the strength of the harmonic confining potential, m is the mass, and a is the s-wave scattering length. We assume a contact interaction since typically the range of the interatomic potential is smaller than the scattering length.

The **filled lattice as a whole** is a quantum many body system which can be described by the Hubbard Hamiltonian (2)

$$H = -J \sum_{\{i,j\},\sigma} c_{i,\sigma}^\dagger c_{j,\sigma} + U \sum_i n_{i,\downarrow} n_{i,\uparrow}.$$

$c_{i,\sigma}^\dagger$ and $c_{i,\sigma}$ are the creation and annihilation operators for an atom with spin $\sigma = \{\uparrow, \downarrow\}$ on lattice site i, $n_{i,\sigma}$ is the occupation number, J is the tunnelling matrix element and U is the on-site interaction strength.

Which tuning knobs do we have in the lattice?

- **Interaction strength**. There exist Feshbach resonances for both s-wave and p-wave interactions. For s-wave interactions the on-site interaction strength can be expressed by $U = 4\pi\hbar^2 a/m \int |\psi(\mathbf{x})|^4 d^3x$, with a being the s-wave scattering length and $\psi(\mathbf{x})$ the wave function of the localized atom.
- **Density/Filling**. Atom number and strength of the external confinement can be (almost) freely chosen.
- **Tunnelling**. The tunnelling rate $J = \frac{4}{\sqrt{\pi}} E_R s^{3/4} e^{-2\sqrt{s}}$ depends directly on the potential depth $V = s\dot{E}_R$ of the optical lattice. $E_R = \hbar^2 k^2/2m$ is the recoil energy with $k = 2\pi/\lambda$ being the wave number of the lattice laser.
- **Dimensionality**. The tunnel coupling can be chosen independently in all three directions of space. Suppressed tunnelling along one axis creates two-dimensional quantum systems, suppressed tunnelling along two axes creates

one-dimensional quantum systems. To reach a low-dimensional configuration the tunnelling matrix element J should be chosen such that the time scale for tunnelling $h/(4J)$ is larger than the experimental time scales.

- **Periodicity/Superlattices/Disorder**. The periodicity of the lattice is determined by the wavelength of the laser and the geometry of the laser beams. Superlattice structures can be generated by overlapping lattices derived from lasers with different wavelengths or adding randomly generated potentials.

II. LOADING FERMIONS INTO AN OPTICAL LATTICE

We create a three-dimensional optical lattice by overlapping three pairs of counter-propagating laser beams.

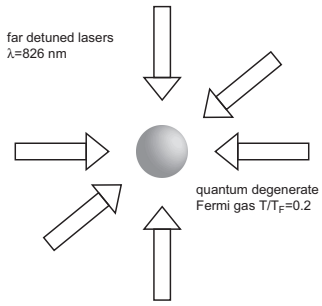

FIG. 2 How to create an optical lattice filled with fermionic atoms (3). For a realization using a single standing wave see (4; 5).

The procedure to prepare fermions in an optical lattice consists of several steps:

1. Prepare a quantum degenerate Fermi gas (^{40}K) t a temperature of $T/T_F = 0.2$ by sympathetic cooling with a bosonic atom cloud (^{87}Rb) in a magnetic trap. After degeneracy is reached, we remove the bosonic atoms.
2. Transfer the Fermi gas into an optical dipole trap and prepare the desired spin states/spin mixture.
3. Turn on the optical lattice. The lasers are far-detuned from the atomic resonance (the lattice lasers operate at $\lambda = 826\,\mathrm{nm}$ whereas the potassium resonance ist at $\lambda = 767\,\mathrm{nm}$). Therefore we can regard the optical lattice as a conservative potential and neglect off-resonant excitation of the atoms by the laser light.

III. IMAGING THE FERMI SURFACE

The potential created by the optical lattice results in a simple cubic crystal structure and the gaussian intensity profiles of the lattice beams give rise to an additional confining potential which varies with the laser intensity. As compared to solid state systems, this gives rise to a harmonic confining potential in addition to the standard Hubbard model:

$$H = -J \sum_{\{i,j\},\sigma} c^\dagger_{i,\sigma} c_{j,\sigma} + U \sum_i n_{i,\downarrow} n_{i,\uparrow} + \sum_{i,\sigma} n_{i,\sigma} \frac{m}{2} \omega_\alpha^2 (id)^2 \tag{1}$$

where ω_α ($\alpha = x, y, z$) denotes the curvature of the harmonic potential and $d = \lambda/2$ is the lattice spacing. As a result, the sharp edges characterizing the $T = 0$ distribution function for the quasi momentum in the homogeneous case (6) are expected to be rounded off. A quantitative picture can be obtained by considering a tight-binding Hamiltonian to describe non-interacting fermions in an optical lattice with an additional harmonic confinement (7). At $T = 0$ the inhomogeneous system is characterized by the total atom number N and by the characteristic length ζ over which the potential shift due to the harmonic confinement equals the tunnel coupling matrix element J (7): $\zeta_\alpha = \sqrt{2J/m\omega_\alpha^2}$. The density distribution scaled by ζ_α and the momentum distribution of the atoms in the lattice only depend on the characteristic density $\rho_c = \frac{Nd^3}{\zeta_x \zeta_y \zeta_z}$ (8).

To observe the Fermi surface of the atoms in the lattice we have measured the quasi-momentum distribution of the atoms. We use adiabatic switch-off of the lattice to convert the quasi-momentum into momentum (see fig.3) which we then observe in time-of-flight imaging (9).

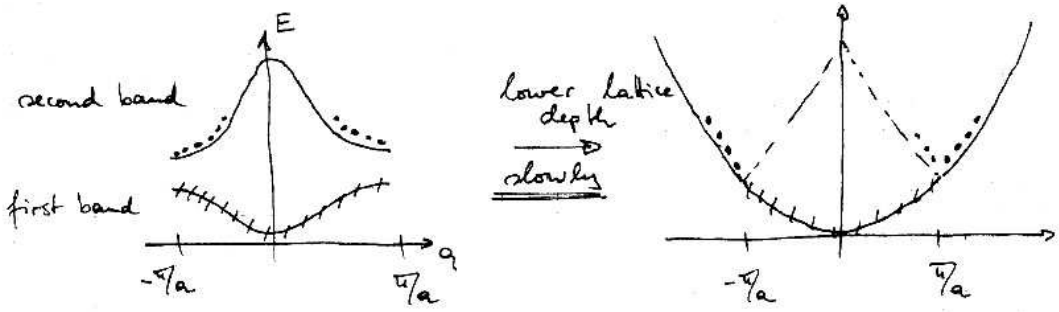

FIG. 3 Detecting the quasi-momentum distribution.

The images show the quasi-momentum distribution of the atoms in the lattice (see fig. 4). Depending on the density of the atoms we realize either a conducting or a band-insulating state. When we increase the characteristic density we observe that the first Brillouin zone gets more and more filled transforming from a conducting into a band-insulating state.

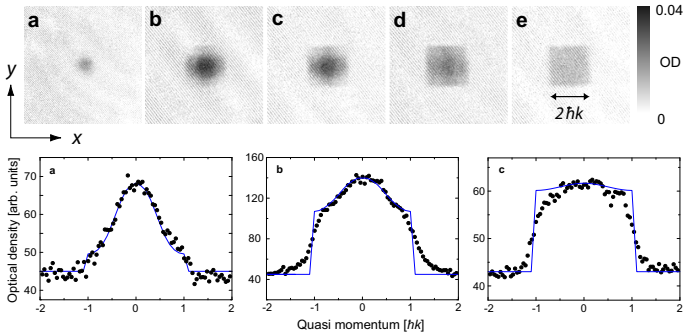

FIG. 4 Transforming the gas from a conducting to a band-insulating state when changing the characteristic density (images taken from (3)). The top row shows absorption images while the bottom row represents horizontal density profiles together with a numerical simulation of the quasi-momentum distribution in the lattice.

In the band insulator tunnelling is prevented by Pauli's exclusion principle since particles have to tunnel into the excited state in the next lattice well (see fig. 5). Therefore the energy gap which prevents the tunnelling is on the order of the trapping frequency inside the individual wells, which is $\approx 2\pi \times 60\,\mathrm{kHz}$. This about 1-2 orders of magnitude larger than the energy gap of a bosonic Mott insulator and the fermions are consequently much better localized.

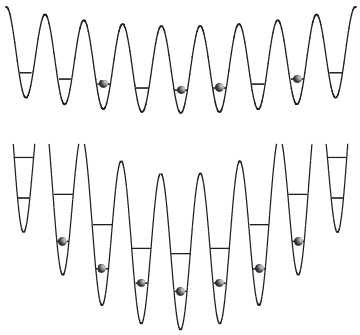

FIG. 5 Conducting (top) vs. band-insulating (bottom) state in the lattice.

IV. DYNAMICS IN THE LATTICE

With ultracold atoms in optical lattices a rapid change of density/filling is possible. We have first created a band insulating state and then lowered the atomic density over a varying time scale (see fig. 6). Thereby the band insulating state develops into a conducting state which we have observed by monitoring the delocalization of the atoms in the lattice. In a conducting state every atom may be delocalized of a few lattice sites and thus after a rapid switch-off of the lattice one observes matter wave interference of these atoms. We determine the coherence length by determining the width of the central momentum peak, or equivalently the width of the quasi-momentum distribution in the first Brillouin zone. In contrast, localized atoms show no interference pattern but the momentum distribution corresponds to the Fourier transform of the localized wave packet.

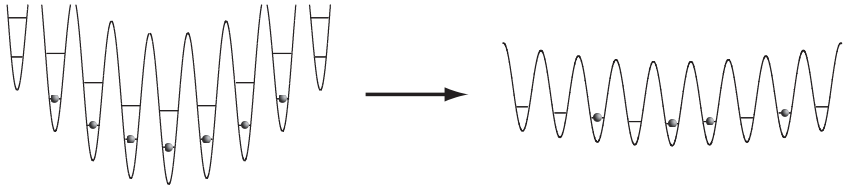

FIG. 6 Transforming a band-insulating into a conducting state

.

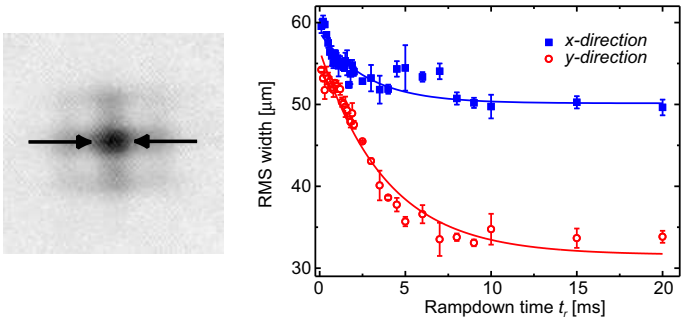

FIG. 7 We determine experimentally whether the state is conducting or band-insulating by measuring the delocalization of atoms in the lattice (figure taken from (3)).

The observed timescale corresponds to approximately $10\hbar/(2zJ)$, i.e. ten times the time scale for tunnelling in the lattice. This about one order of magnitude slower than for bosonic atoms when returning from a Mott insulator into a superfluid state (10).

V. INTERACTING FERMIONS

In the following we will consider interacting fermions in an optical lattice, specifically two fermions with different spins (see fig.8). Two particles interacting via s-wave interactions (modelled by a δ-functional interaction) in a harmonic trap with trapping frequency ω have been studied by Busch *et al.* (1). Note, that only s-wave ($\ell = 0$) states of the relative coordinates contribute to this interaction. The energy spectrum (see fig. 9) is related to the scattering length a by

$$\sqrt{2}\frac{\Gamma(-E/2\hbar\omega + 3/4)}{\Gamma(-E/2\hbar\omega + 1/4)} = \frac{a_{ho}}{a}, \tag{2}$$

where $a_{ho} = \sqrt{\hbar/m\omega}$ denotes harmonic oscillator ground state extension. For $a = 0$ one recovers the energy eigenvalues of the relative motion of two particles in a three-dimensional harmonic oscillator $E = (2n+\ell+3/2)\hbar\omega = (2n+3/2)\hbar\omega$.

What happens when we sweep the magnetic field across the Feshbach resonance from the repulsive towards the attractive side? When using this direction of the sweep there is no adiabatic conversion to molecules but we transfer atoms from the ground state into the excited state (see fig. 10).

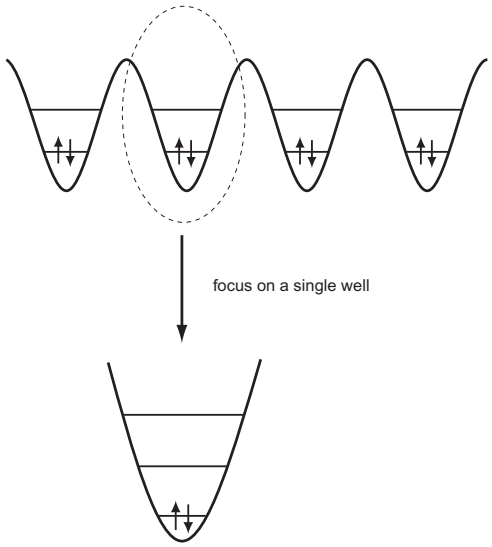

FIG. 8 A band insulator with two species can be considered as many copies of two atoms in a harmonic potential well.

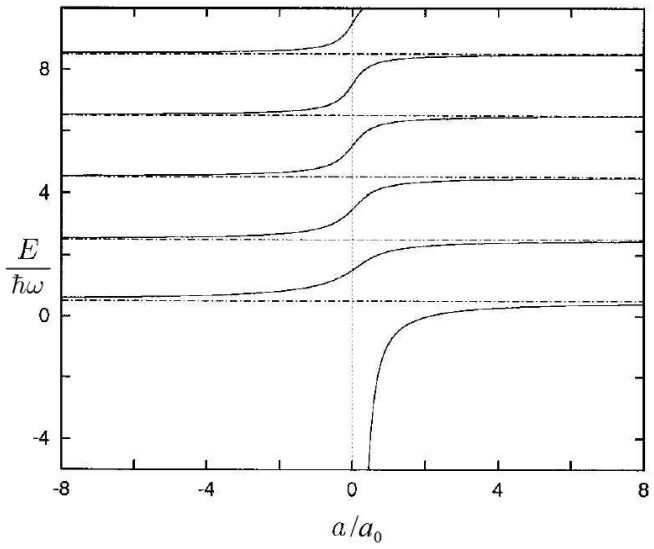

FIG. 9 Energy spectrum of two interacting particles in a harmonic potential well (figure taken from (1)).

After turning off the optical lattice adiabatically and switching off the magnetic field we measure the momentum distribution. To see the effect of the interactions we determine the fraction of atoms transferred into higher bands. For final magnetic field values well above the Feshbach resonance we observe a significant increase in the number of atoms in higher bands along the weak axis of the lattice, demonstrating an interaction-induced coupling between the lowest bands. Since the s-wave interaction is changed on a time scale short compared to the tunnelling time between adjacent potential minima we may regard the band insulator as an array of harmonic potential wells. It has been shown that increasing the s-wave scattering length for two particles in a harmonic oscillator shifts the energy of the two-particle state upwards until the next oscillator level is reached (1). In our case this leads to a population of higher energy bands. The fraction of atoms transferred could be limited by the number of doubly occupied lattice sites and tunnelling in the higher bands. The number of doubly occupied sites could be measured by studying the formation of molecules in the lattice. In addition, we observe a shift of the position of the Feshbach resonance from its value in free space to larger values of the magnetic field (see Fig. 4a), which has been predicted for tightly confined atoms in an optical lattice (11). This mechanism for a confinement induced resonance is related to the phenomenon

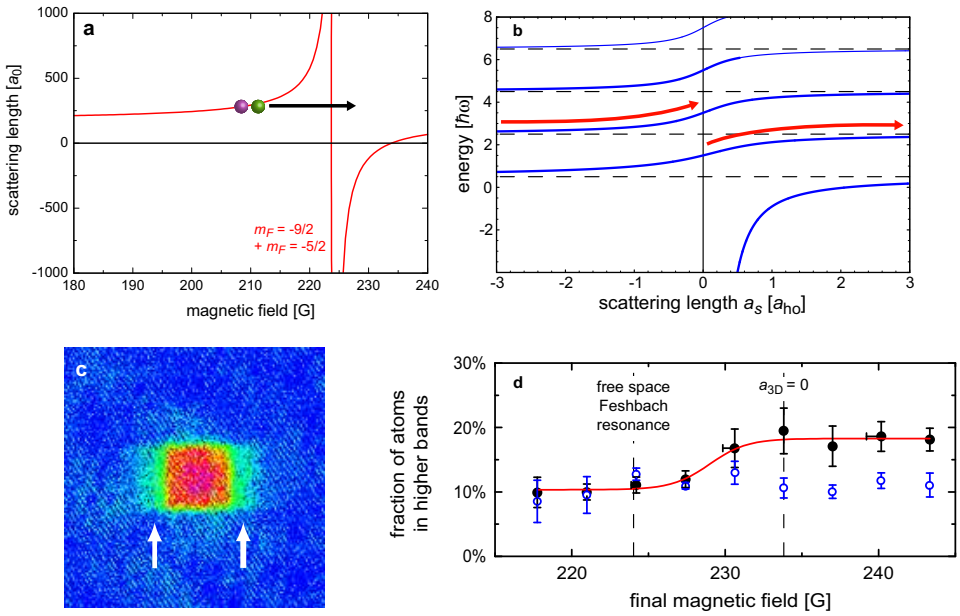

FIG. 10 Coupling of different Bloch bands by sweeping the magnetic field across a Feshbach resonance from the low-field to the high-field side. **a** Sweep direction. **b** Evolution of the energy eigenvalues when the scattering length is changed. **c** Observation of atom in higher bands. **d** Fraction of atoms transferred into higher band depending on the final value of the magnetic field sweep (figure c and d are taken from (3)).

predicted (12; 13) and observed (14) for one-dimensional quantum gases. For a quantitative description of this strongly interacting Fermi gas on a lattice a multi-band Hubbard model could be considered but these are even in the static case notoriously difficult or even impossible to solve with present methods (15).

VI. MOLECULES IN A 3D OPTICAL LATTICE

Reversing the direction of the sweep produces molecules in the optical lattice. Two atoms residing at a given lattice site are adiabatically converted into a bound pair of atoms. We probe the molecules by RF spectroscopy (16). We drive an RF transition between the $|F = 9/2, m_F = -7/2\rangle$ and the $|F = 9/2, m_F = -5/2\rangle$ states. If a bound state between an atom in the $|F = 9/2, m_F = -9/2\rangle$ and $|F = 9/2, m_F = -7/2\rangle$ exists, the transition frequency is altered by the binding energy.

We observe the binding energy of the molecules inside the optical lattice to differ from the free space situation. In particular we find bound states even for a negative scattering length. This effect is characteristic for low dimensional systems:

- **2D:** Predicted by Petrov *et al.* (17) and Wouters *et al.* (18).
- **1D**: Predicted by Maxim Olshanii and co-workers (12; 13), observed with fermions in an optical lattice (14) (see below).
- **"0"D** (atoms localized in a three-dimensional lattice): The theory by Busch *et al.* (1) fits well to our data.

The shift is due to the confining potential, which lifts the continuum to the ground state of the external potential. Therefore a quasi-bound state with negative scattering length which initially was above the free-space continuum is now below the new "continuum" set the confining potential.

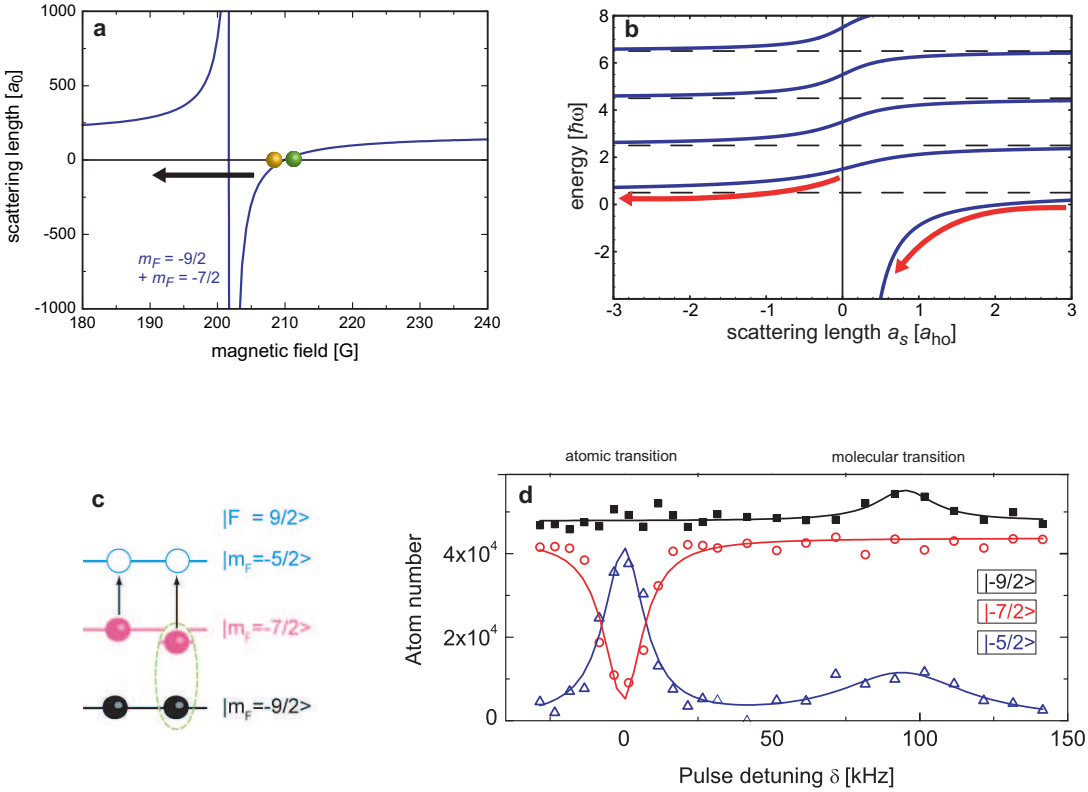

FIG. 11 Generation of molecules in the optical lattice by sweeping the magnetic field across a Feshbach resonance from the high-field to the low-field side. **a** Sweep direction. **b** Evolution of the energy eigenvalues when the scattering length is changed. **c** Principle of the spectroscopy to measure the binding energy of the atoms. **d** Sample spectrum.

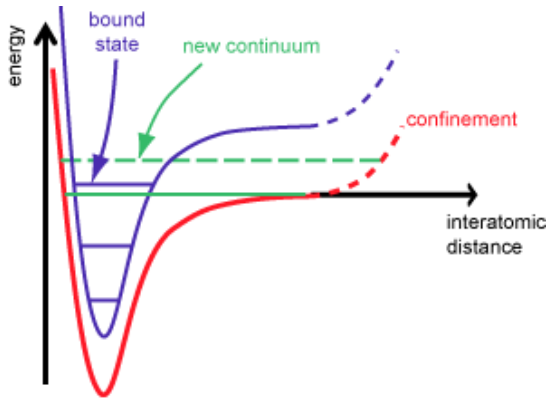

FIG. 12 Confinement induced bound states.

VII. CONFINEMENT INDUCED MOLECULES IN A 1D FERMI GAS

The study of two particles forming a bound state has a long history both in physics and chemistry because it constitutes the most elementary chemical reaction. In most situations, such as atoms in the gas phase or in a liquid, the two particles can be considered as being in free space and their collisions can be described by standard quantum mechanical scattering theory. For ultracold atoms undergoing s-wave interaction a bound molecular state is only supported when the scattering length between the atoms is positive whereas for negative scattering length the bound state is absent (19).

Tight transverse confinement alters the scattering properties of two colliding atoms fundamentally and a bound state exists irrespective of the sign of the scattering length. This peculiar behaviour in a one-dimensional system arises

from the additional radial confinement which raises the continuum energy to the zero point energy of the confining potential, e.g. the two-dimensional harmonic oscillator ground state energy $\hbar\omega_r$. The energy of a bound or quasi-bound state remains nearly unaffected by the external confinement as long as the effective range of the interaction is small compared to the extension of the confined ground state. Therefore, a quasi-bound state, which for negative scattering length a lies above the continuum in free space, is below the new continuum in the confined system.

The binding energy E_B of dimers in a one-dimensional gas is given by (13)

$$\frac{a}{a_r} = -\frac{\sqrt{2}}{\zeta(1/2, -E_B/2\hbar\omega_r)}, \tag{3}$$

where $a_r = \sqrt{\hbar/m\omega_r}$ is the extension of the transverse ground state (with m being the atomic mass) and ζ denotes the Hurwitz zeta function. For negative a and $|a| \ll a_r$ a weakly bound state with $E_B \approx m\omega_r^2 a^2$ exists which has a very anisotropic shape (20). In the limit $|a| \gg a_r$ the binding energy takes the universal form $E_B \approx 0.6\,\hbar\omega_r$ and for positive a and $a \ll a_r$ the usual 3D expression for the binding energy $E_B = \hbar^2/ma^2$ is recovered.

A trapped gas is kinematically one-dimensional if both the chemical potential and the temperature are smaller than the level spacing due to the transverse confinement. For a harmonically trapped Fermi gas the Fermi energy $E_F = N \cdot \hbar\omega_z$ must be smaller than the energy gap to the first excited state in the transverse direction $\hbar\omega_r$. N denotes the number of particles and ω_z is the trapping frequency along the weakly confining axis. In our experiment we employ a two-dimensional optical lattice in order to create 1D Fermi gases. For atoms trapped in the intensity maxima of the two perpendicular standing wave laser fields the radial confinement is only a fraction of the optical lattice period (9). The much weaker axial trapping is a consequence of the gaussian intensity envelope of the lattice laser beams. The resulting aspect ratio $\frac{\omega_r}{\omega_z} = \frac{\pi w}{\lambda}$ is determined by the waist w and the wavelength λ of the beams. The two-dimensional optical lattice creates an array of 1D tubes of which approximately 70×70 are occupied (21). This array fulfills the 1D condition $N < \omega_r/\omega_z \approx 270$ in each tube while simultaneously providing a good imaging quality.

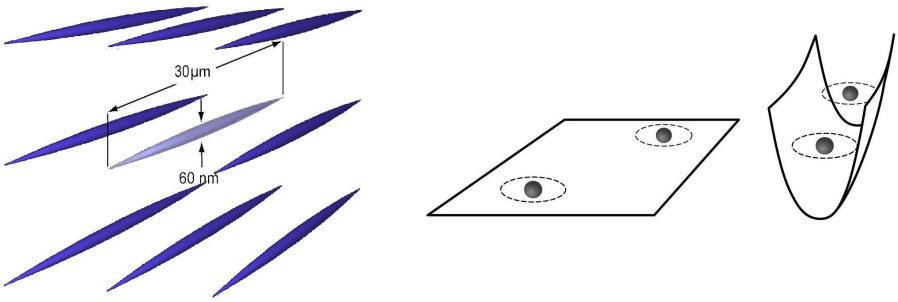

FIG. 13 One-dimensional Fermi gases in a three-dimensional optical lattice (left). Illustration of the one-dimensional scattering process where strongly interacting atoms cannot pass each other, whereas in two dimensions they can (right).

We have measured the binding energy of the molecules by RF spectroscopy and have investigated the dependence of the binding energy of the 1D dimers on the magnetic field (Fig.14). We observed bound states for every examined magnetic field strength. The dimers at magnetic fields above the Feshbach resonance are induced by the confinement. The data is in good agreement with the theoretical expectation calculated from Eq. 3 (solid line) with no free parameters. For this calculation we compute the effective harmonic oscillator length a_r and the ground state energy $\hbar\omega_r$ by minimizing the energy of a gaussian trial wave function in a single well of the lattice to account for the anharmonicity of the potential. To calculate the scattering length we use a width of the Feshbach resonance of $\Delta B = 7.8\,\mathrm{G}$ (22) and background scattering length $a_{bg} = 174\,a_0$ (23).

For a comparison with the situation in free space we created molecules in a crossed beam optical dipole trap without optical lattice where confinement effects are not relevant. The binding energy in 3D is measured with the same rf spectroscopy technique as for the 1D gas and we find molecules only for scattering lengths $a > 0$. The binding energy is calculated according to (24) as $E_{B,3D} = \frac{\hbar^2}{m(a-\bar{a})^2}$ with $\bar{a} = (mC_6/\hbar^2)^{1/4}\frac{\Gamma(3/4)}{2\sqrt{2}\Gamma(5/4)}$ being the effective scattering length and $C_6 = 3897$ (in atomic units) (25). The deviation of the theory from the measured data for more deeply bound molecules is probably due to limitations of this single channel theory. A multi-channel calculation would determine the binding energy more accurately.

Exactly on the Feshbach resonance where the scattering length diverges, the binding energy takes the universal form $E_B \approx 0.6\hbar\omega_r$ and is solely dependent on the external confinement. We have varied the potential depth of the

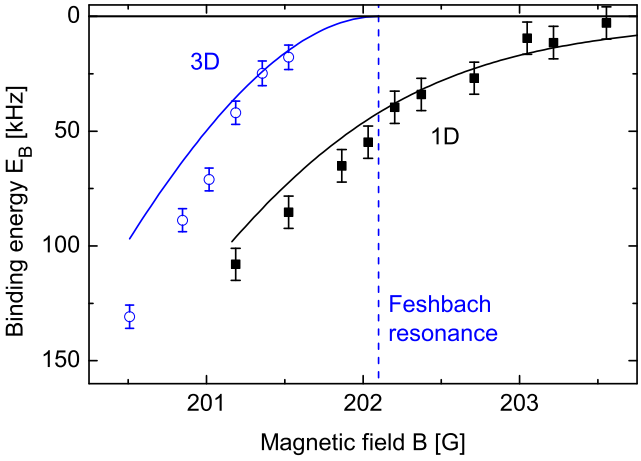

FIG. 14 1D and 3D molecules. Confinement induced molecules in the 1D geometry exist for arbitrary sign of the scattering length. The solid lines show the theoretical prediction of the binding energy with no free parameters (see text). In the 3D case we observed no bound states at magnetic fields above the Feshbach resonance (vertical dashed line). The error bars reflect the uncertainty in determining the position of the dissociation threshold (figure taken from (14)).

optical lattice and thereby the transverse confinement and measured the binding energy. We find good agreement of our data with the theoretical prediction (see Fig. 15). For a very low depth of the optical lattice the measured data deviate from the 1D theory due to the fact that the gas is not one-dimensional anymore.

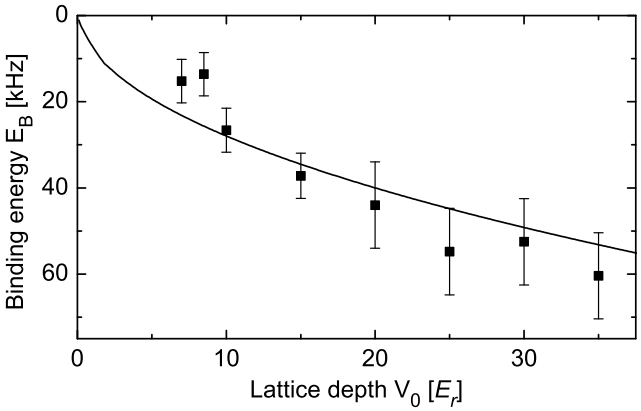

FIG. 15 Changing the confinement. The plot shows the binding energy very close to the Feshbach resonance at a magnetic field of $B = 202.0\,\mathrm{G}$. The error bars reflect the uncertainty in determining the position of the dissociation threshold. The solid line shows the theoretically expected value $E_B = 0.6\,\hbar\omega_r$ (figure taken from (14)).

VIII. CONCLUSIONS

Fermions in an optical lattice offer a versatile tool to study few- and many-body physics. Our recent results about fermions in an optical lattice can be found in the references (3; 14).

References

[1] T. Busch, B.-G. Englert, K. Rzazewski, M. Wilkens, Found. Physics **28**, 549 (1998).
[2] J. Hubbard, Proc. R. Soc. Lond. A **276**, 238 (1963).
[3] M. Köhl, H. Moritz, T. Stöferle, K. Günter, T. Esslinger, Phys. Rev. Lett. **94**, 080403 (2005).

[4] G. Modugno, F. Ferlaino, R. Heidemann, G. Roati, M. Inguscio, Phys. Rev. A **68**, 011601 (2003).
[5] S. Jochim *et al.*, Phys. Rev. Lett. **91**, 240402 (2003).
[6] N. W. Ashcroft and N. D. Mermin, *Solid States Physics*, Saunders College Publishing, 1976.
[7] M. Rigol, A. Muramatsu, Phys. Rev. A **69**, 053612 (2004)
[8] M. Rigol, A. Muramatsu, G. G. Batrouni, R. T. Scalettar, Phys. Rev. Lett. **91**, 130403 (2003)
[9] M. Greiner, I. Bloch, O. Mandel, T.W. Hänsch, T. Esslinger, Phys. Rev. Lett. **87**, 160405 (2001).
[10] M. Greiner, O. Mandel, T. Esslinger, T.W. Hänsch, I. Bloch, Nature **415**, 39 (2002).
[11] P. O. Fedichev, M. J. Bijlsma, P. Zoller, Phys. Rev. Lett. **92**, 080401 (2004).
[12] M. Olshanii, Phys. Rev. Lett. **81**, 938 (1998).
[13] T. Bergeman, M. G. Moore, M. Olshanii, Phys. Rev. Lett. **91**, 163201 (2003).
[14] H. Moritz, T. Stöferle, K. Günter, M. Köhl, T. Esslinger, Phys. Rev. Lett. **94**, 210401 (2005).
[15] M. Troyer, U. Wiese, Phys. Rev. Lett. **94**, 170201 (2005)
[16] C. A. Regal, C. Ticknor, J. L. Bohn, and D. S. Jin, Nature **424**, 47 (2003).
[17] D. S. Petrov, M. Holzmann, G.V. Shlyapnikov, Phys. Rev. Lett. **84**, 2551 (2000).
[18] M. Wouters, J. Tempere, J. T. Devreese, Phys. Rev. A **68**, 053603 (2003).
[19] E. Wigner, Zeitschr. f. Physik **83**, 253 (1933).
[20] I. V. Tokatly, Phys. Rev. Lett. **93**, 090405 (2004).
[21] For a noninteracting gas in the lattice trap we measure $1/e^2$ cloud diameters of approximately $60\,\mu$m along the tube axis and $35\,\mu$m radially.
[22] C. A. Regal, M. Greiner, and D. S. Jin, Phys. Rev. Lett. **92**, 083201 (2003).
[23] C. A. Regal, and D. S. Jin, Phys. Rev. Lett. **90**, 230404 (2003).
[24] G. F. Gribakin, and V. V. Flambaum, Phys. Rev. A **48**, 546 (1993).
[25] A. Derevianko, W. R. Johnson, M. S. Safronova, J.F. Babb, Phys. Rev. Lett. **82**, 3589 (1999).